Carcinogenesis vol.34 no.10 pp.2206–2217, 2013
doi:10.1093/carcin/bgt182
Advance Access publication May 28, 2013

Glycogen synthase kinase 3β inhibition sensitizes human glioblastoma cells to temozolomide by affecting O^6-methylguanine DNA methyltransferase promoter methylation via c-Myc signaling

Ilya V.Pyko[1,2], Mitsutoshi Nakada[1,*], Hemragul Sabit[1], Lei Teng[1,3], Natsuki Furuyama[1], Yutaka Hayashi[1], Kazuyuki Kawakami[4], Toshinari Minamoto[4], Aliaksandr S.Fedulau[2] and Jun-ichiro Hamada[1]

[1]Department of Neurosurgery, Division of Neuroscience, Graduate School of Medical Science, Kanazawa University, 13-1 Takara-Machi, 920-8641, Kanazawa, Ishikawa, Japan, [2]Department of Neurology and Neurosurgery, Belarusian State Medical University, Dzerzhynskogo Prospect 83, 220116, Minsk, Belarus, [3]Department of Neurosurgery, The First Clinical College of Harbin Medical University, Nangang, Harbin 150001, China and [4]Division of Translational and Clinical Oncology, Cancer Research Institute, Kanazawa University, 13-1 Takara-Machi, 920-0934, Kanazawa, Ishikawa, Japan

*To whom correspondence should be addressed. Tel: +81 76 265 2384; Fax: +81 76 234 4262;
Email: mnakada@med.kanazawa-u.ac.jp

Glycogen synthase kinase 3β (GSK3β) is a serine/threonine protein kinase involved in human cancers including glioblastoma. We have previously demonstrated that GSK3β inhibition enhances temozolomide effect in glioma cells. In this report, we investigated the molecular mechanisms of sensitization of glioblastoma cells to temozolomide by GSK3β inhibition, focusing on O^6-methylguanine DNA methyltransferase (MGMT) gene silencing. Glioblastoma tissues from patients treated with the GSK3β-inhibiting drugs were subjected to immunohistochemistry and methylation-specific PCR assay. Human glioblastoma cell lines T98G, U138, U251 and U87 were treated with a small-molecule GSK3β inhibitor, AR-A014418 or GSK3β-specific small interfering RNA. The combined effect of temozolomide and AR-A014418 on cell proliferation was determined by AlamarBlue assay and an isobologram method. MGMT promoter methylation was estimated by methylation-specific PCR and MethyLight assay. MGMT gene expression was evaluated by real-time quantitative reverse transcriptase-PCR. c-Myc and DNA (cytosine-5)-methyltransferase 3A binding to the MGMT promoter was estimated by chromatin immunoprecipitation assay. GSK3β inhibition decreased phosphorylation of glycogen synthase and reduced MGMT expression and increased MGMT promoter methylation in clinical tumors. In glioblastoma cell lines, GSK3β inhibition decreased cell viability, enhanced temozolomide effect and downregulated MGMT expression with relevant changes in the methylation levels of the MGMT promoter. Here, we showed for the first time that c-Myc binds to the MGMT promoter with consequent recruitment of DNA (cytosine-5)-methyltransferase 3A, regulating the levels of MGMT promoter methylation. The results of this study suggest that GSK3β inhibition enhances temozolomide effect by silencing MGMT expression via c-Myc-mediated promoter methylation.

Introduction

Glioblastoma (GBM) is the most frequent malignant tumor of the brain and is highly unresponsive to the currently available anticancer treatments. The proliferative and invasive activity of GBM (1) hinders curable surgical intervention and makes GBM highly resistant to radiation and chemotherapy (2) with median patient survival showing little improvement over the past 30 years (3). Consequently, there is an urgent need to develop new treatment modalities represented by molecular target-directed therapies (4,5).

O^6-methylguanine DNA methyltransferase (MGMT) promoter methylation is an independent favorable prognostic factor in patients with GBM (6). The levels of MGMT gene promoter methylation are associated with MGMT expression and are important in setting the transcriptional state of the MGMT promoter through changes in chromatin structure (7). Although the MGMT promoter is methylated only in 22% of GBM cases, methylation status of the promoter is implicated in chemosensitivity to temozolomide (TMZ) (6). Therefore, patients with a methylated MGMT promoter may benefit from TMZ therapy (6).

Glycogen synthase kinase 3β (GSK3β) is a multifunctional protein kinase that regulates various cellular pathways depending on its substrates for phosphorylation (8). We have shown that deregulated GSK3β expression and activity maintains survival and proliferation and that GSK3β-specific inhibitors suppress survival and proliferation and induce apoptosis in human GBM cells (9,10). We have also demonstrated that GSK3β inhibition significantly sensitized GBM cell lines to TMZ (10). Based on our research, we are conducting clinical research for the therapeutic effect of GSK3β inhibition in recurrent GBM.

Here, we investigated the molecular mechanisms underlying a combined effect of GSK3β inhibition with TMZ, focusing on MGMT gene silencing and its causal relationship with c-Myc signaling, which is known to be upregulated by GSK3β inhibition (11,12). The results suggest that GSK3β inhibition enhances TMZ effect by decreasing MGMT expression via its c-Myc-mediated promoter methylation.

Material and methods

Clinical tumor samples and histological examination

In our institute, clinical research entitled 'Chemotherapy for recurrent malignant glioma with combined usage of temozolomide and GSK3β-inhibiting drugs' is ongoing under the approval by the Medical Ethics Committee of Kanazawa University Hospital (UMIN Clinical Trial Registry: UMIN000005111). According to the institutional review board-approved protocol, fresh GBM tissues were obtained at surgery and/or autopsy. The histological diagnosis of tumor was determined according to the revised World Health Organization criteria (13). In seven patients registered for the trial, autopsy was available for three patients with obtained informed consent from their families and was performed 2 h after death. Patients 1 and 2 underwent administration of GSK3β-inhibiting drugs until death with last administration within 8 h antemortem. One patient stopped GSK3β-inhibiting drugs 3 months prior to death. Patients 1 and 3 died from cerebrospinal fluid dissemination of GBM. Histology did not differ between the primary tumor and the recurrent tumor obtained by autopsy. In patient 2, the primary brain stem tumor tissues obtained by needle biopsy were diagnosed with GBM. This patient died from enlargement of the brain stem lesion. The autopsy specimens showed the presence of GBM. All tumor samples obtained were fixed in neutral-buffered 10% formalin and were embedded in paraffin. The detailed information and outcome of this clinical research will be submitted elsewhere.

Immunohistochemistry

Immunohistochemistry was performed for the clinical tumor tissues as described previously (14). Briefly, formalin-fixed and paraffin-embedded tissue blocks were sectioned (6 μm thick) onto slides and then deparaffinized. Sections were immunostained using an Envision+ Kit (Dako, Tokyo, Japan) with anti-glycogen synthase polyclonal antibody, anti-phospho-glycogen synthase polyclonal antibody specific to serine (S) 641-phosphorylated glycogen synthase (p-GS^{S641}) and anti-MGMT antibody (Cell Signaling

Abbreviations: ChIP, chromatin immunoprecipitation; DMSO, dimethyl sulfoxide; DNMT3A, DNA (cytosine-5)-methyltransferase 3A; EGS, ethylene glycol bis(succinimidylsuccinate); GBM, glioblastoma; GS, glycogen synthase; GSK3β, glycogen synthase kinase 3β; MGMT, O^6-methylguanine DNA methyltransferase; MSP, methylation-specific PCR; p-GS^{S641}, serine (S) 641-phosphorylated glycogen synthase; qPCR, quantitative real-time PCR; QRT–PCR, quantitative reverse transcriptase–polymerase chain reaction; siRNA, small interfering RNA; TMZ, temozolomide.

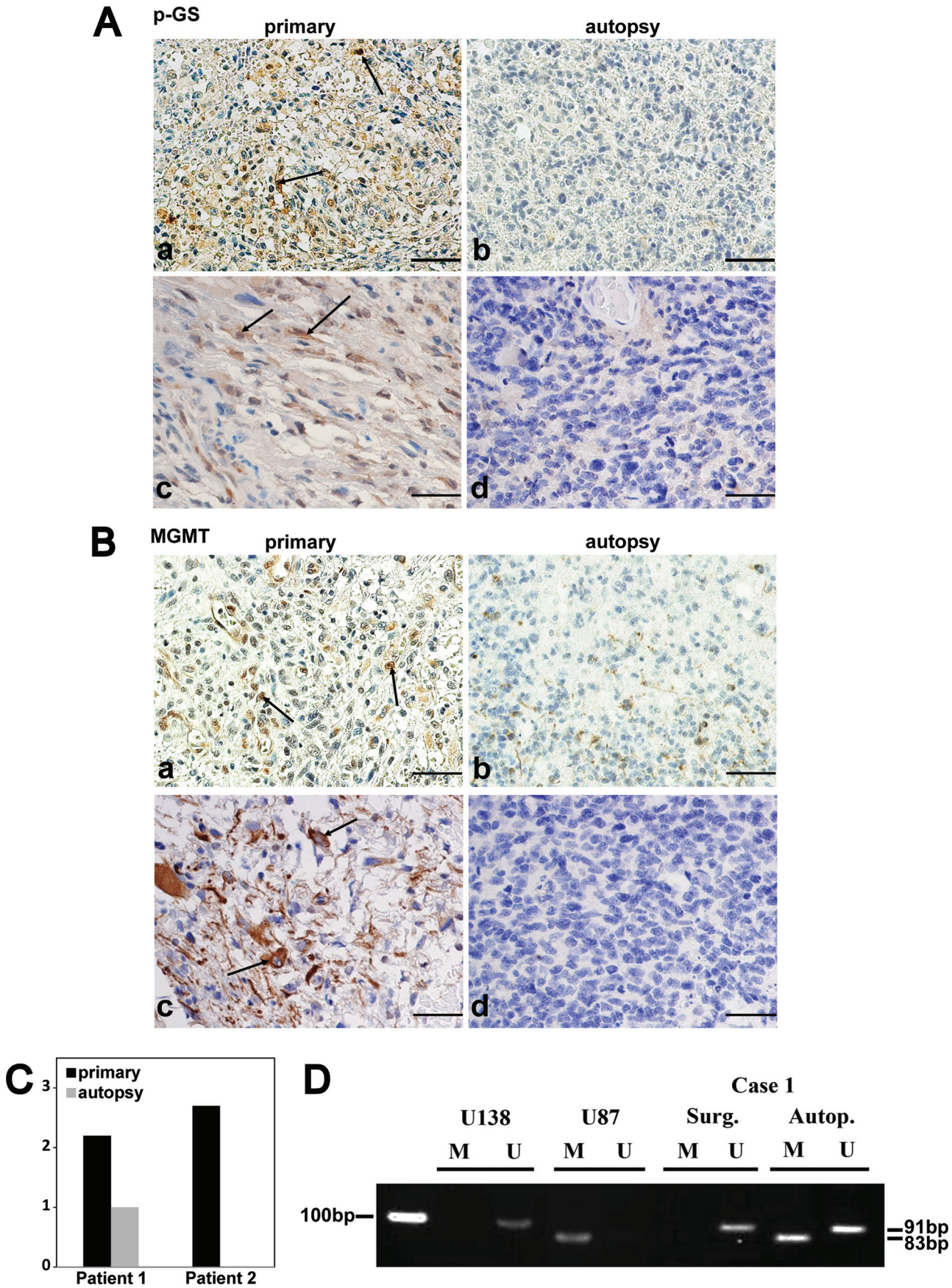

Fig. 1. (**A**) The immunohistochemical localization of phosphorylated GS in tissues. a and b, patient 1; c and d, patient 2; a and c, primary tumor; b and d, the GSK3β-inhibiting drug-treated recurrent tumor obtained at autopsy. Paraffin sections were immunostained with the antibody against p-GS^{S641}. Note that

Technology, Danvers, MA) using a 1:200 dilution. Sections were microwaved for 15 min in target retrieval solution (pH 9.0; Dako), blocked by incubation in 0.3% H_2O_2 solution in methanol for 20 min. Non-specific immunoreactions were blocked at room temperature for 30 min using a Protein-Block Kit (Dako). Slides were incubated with rabbit anti-p-GS^{S641} antibody, anti-glycogen synthase antibody or rabbit anti-MGMT antibody overnight at 4°C, and they were washed and secondary antibody was applied for 30 min. Sections were exposed to diaminobenzidine peroxidase substrate (Funakoshi) for 3–5 min and counterstained with Mayer's hematoxylin. Non-immune rabbit IgG (Sigma–Aldrich, St Louis, MO) was used as a negative control.

DNA extraction

After microscopic observation of hematoxylin and eosin-stained sections by a neuropathologist (H.S.), DNA was extracted from the tumor areas of formalin-fixed and paraffin-embedded tissue samples of patient 1 by using a QIAamp DNA Mini Kit™ (Qiagen, GmbH, Hilden, Germany). The amount of the sample obtained by needle biopsy in patient 2 was not enough for DNA extraction.

Cell cultures

Human GBM cell lines T98G, U138, U251 and U87 were obtained from the American Type Culture Collection (Manassas, VA). Cell lines were maintained in Dulbecco's modified Eagle's medium supplemented with 10% fetal bovine serum both from GIBCO (Grand Island, NY) at 37°C and 5% CO_2.

Effects of GSK3β inhibitors on tumor cells

GBM cells were serum starved for 24 h and seeded in the cell proliferation assay format, as detailed elsewhere (15–17). Briefly, cells were seeded in 96-well plastic plates and treated with dimethyl sulfoxide (DMSO) as a vehicle control or with a small-molecule GSK3β inhibitor AR-A014418 (Sigma) dissolved in equivalent amount of DMSO at escalating final concentrations (5–80 μmol/l). Medium was replaced after 72 h of incubation in all treatment and control wells with the medium of the same formulation (containing the same final concentration of AR-A014418) (17). The proliferation assay was performed by adding AlamarBlue (AbD Serotec, Kidlington, UK) to the cells 144 h after cell seeding to assess proliferation according to the manufacturer's protocol. Absorbance values were measured by spectrophotometry using a Microplate Reader Model 550 (Bio-Rad, Hercules, CA) at 540 and 590 nm. The relative cell viability was determined by calculated values of the percent difference in reduction of AlamarBlue between treated and control cells as described in the manufacturer's protocol. The experiments were carried out in sextuplicates.

RNA interference

GBM cells seeded into 96-well plates were transfected with small interfering RNA (siRNA) specific to human GSK3β (target sequence, 5′-GCUCCAGAUCAUGAGAAAGCUAGAU-3′) proved to be effective in glioma cells in our previous study (10) or negative control siRNA (Stealth RNAi Negative Control Low GC duplex) both from Invitrogen (Grand Island, NY), or β-catenin-specific siRNA (Cell Signaling Technology). Lipofectamine RNAiMAX (Invitrogen) was used for transfection according to the manufacturer's protocol. The relative cell viability was determined 72 h after incubation by the AlamarBlue assay.

Western blot analysis

Western blot analysis was performed on polyvinylidene difluoride membrane (Invitrogen), according to the standard procedure as described previously (14,16). Rabbit monoclonal anti-c-Myc antibody (Epitomics, Burlingame, CA), mouse monoclonal anti-GSK3β antibody and mouse monoclonal anti-tyrosine 216-phosphorylated GSK3β antibody (BD Biosciences, San Jose, CA), anti-DNA (cytosine-5)-methyltransferase 3A antibody (Imgenex, San Diego, CA), anti-β-catenin antibody and anti-MGMT antibody (Cell Signaling Technology) were used at a dilution of 1:5000, 1:10 000, 1:5000, 1:1000, 1:5000 and 1:2500, respectively.

Effect of GSK3β inhibition on the sensitivity of GBM cells to TMZ

After serum starvation for 24 h, GBM cells were seeded in the cell proliferation assay format. The cells were treated with DMSO (vehicle control), with escalating concentrations (50, 100, 200 and 400 μmol/l) of TMZ (Sigma), AR-A014418 (5, 10 and 20 μmol/l) or the combinations of indicated concentrations of TMZ and AR-A014418 dissolved in equivalent amount of DMSO. After treatment for 144 h, cells were subjected to the AlamarBlue assay to determine the dose-dependent effect and IC50 of TMZ and AR-A014418 against GBM cells and to observe the influence of AR-A014418 (5, 10 or 20 μmol/l) on TMZ effect against GBM cells. The influence of GSK3β inhibition on TMZ effect against GBM cells was analyzed using classic isobologram method (18) and median dose-effect analysis (19,20). The IC_{50} values and combination indices of the combination therapy by various concentrations of TMZ and AR-A014418 were plotted to determine whether the effect of GSK3β inhibitor on GBM cell sensitivity to TMZ was additive, synergistic or antagonistic.

Methylation-specific PCR assay

Isolated effect of GSK3β inhibition and combined influence of GSK3β and c-Myc inhibition on methylation status of the MGMT promoter were evaluated by methylation-specific PCR (MSP) assay as described previously (21,22). T98G, U251 and U138 cells were serum starved for 24 h and then treated with DMSO (control) or AR-A014418 (5, 10 or 20 μmol/l) or combination of DMSO–AR-A014418 (5, 10 or 20 μmol/l) and c-Myc inhibitor 20 μmol/l (EMD Millipore, Billerica, MA) dissolved in equivalent amount of DMSO. After treatment for 72 h, genomic DNA was extracted from the cells using a QIAamp DNA Mini Kit (Qiagen). Sodium bisulfite conversion of 200 ng of the purified DNA was performed using an EpiTect Bisulfite Kit (Qiagen) according to the manufacturer's protocol. MSP of bisulfate-converted DNA was carried out in a nested, two-stage PCR approach as described previously (22) using GeneAmp PCR System 2700 (Applied Biosystems, Grand Island, NY). U87 and U138 cell lines were used as methylated and unmethylated controls, respectively. Amplified PCR products were separated by 3% agarose gel electrophoresis and visualized with ethidium bromide.

MethyLight assay

T98G, U251 and U138 cells were serum starved for 24 h and then treated with DMSO (control) or escalating concentrations of AR-A014418 (5, 10 or 20 μmol/l) dissolved in equivalent amount of DMSO or combination of DMSO–AR-A014418 (5, 10 or 20 μmol/l) and c-Myc inhibitor 20 μmol/l. After treatment for 72 h, genomic DNA was extracted from the cells using a QIAamp DNA Mini Kit and subjected to bisulfite conversion using an EpiTect Bisulfite Kit followed by quantitative real-time PCR (qPCR) of bisulfite-converted DNA using PCR premix TaKaRa ExTaq (TaKaRa, Otsu, Japan) with primers and probe specific to methylated fraction of the MGMT promoter. Probe and forward primer sequences were taken from other study (23): probe, 6FAM-CCTTACCTCTAAATACCAACCCCAAACCCG-BHQ-1; forward primer, 5′-CTAACGTATAACGAAAATCGTAACAACC-3′; reverse primer designed by authors, 5′-AGTATGGAAGGGTAGGAAGAATTCG-3′. Alu was utilized as a calibrator (24) with following probe and primers: probe, 6FAM-CCTACCTTAACCTCCC-BHQ-1; forward primer, 5′-GGTTAGGTATAGTGGTTTATATTTGTAATTTTAGTA-3′; reverse primer, 5′-ATTAACTAAACTAATCTTAAACTCCTAACCTCA-3′. The qPCR was performed using LightCycler 1.5 (Roche Diagnostics GmbH, Mannheim, Germany) with protocol consisting of an initial denaturation step at 95°C for 30 s followed by 40 cycles of 95°C for 15 s and 60°C for 60 s. LightCycler Software 4.1 was used to analyze the qPCR data. Threshold cycle values (Ct) were determined and relative methylation of the MGMT promoter was calculated using the ΔC_T method described by the manufacturer using Alu as a calibrator gene.

Real-time quantitative reverse transcriptase–polymerase chain reaction

T98G, U251 and U138 cells were serum starved for 24 h and then treated with DMSO (control) or escalating concentrations of AR-A014418 (5, 10 or 20 μmol/l) dissolved in equivalent amount of DMSO. After treatment for 72 h, total RNA was isolated from the cells using a GenElute Mammalian Total RNA Miniprep Kit (Sigma). Complementary DNA was synthesized from total RNA using a High

←
phosphorylation of GS is found in the cells of primary tumors (arrows), whereas faint staining is observed in the recurrent tumors obtained at autopsy. Cell nuclei were counterstained with hematoxylin. Scale bars, 50 μm. (**B**) The immunohistochemical expression of MGMT protein in the tumor tissues. a and b, patient 1; c and d, patient 2; a and c, primary tumor; b and d, the GSK3β-inhibiting drug-treated recurrent tumor obtained at autopsy. Cells with nuclear staining were considered as positive for MGMT expression (arrows). Cell nuclei were counterstained with hematoxylin. Scale bars, 50 μm. (**C**) Staining intensity of glioma cells was scored individually for MGMT antibody in each specimen and was classified as no (0), weak (1), moderate (2) or strong staining (3); mean staining intensity was calculated separately for primary specimen and autopsy specimen in patients 1 and 2. (**D**) MSP assay for methylation status of the MGMT promoter in GBM cells and the primary and recurrent tumors of the patients. PCR products in the M lanes and U lanes indicate methylated and unmethylated status of the MGMT promoter, respectively. U138, U138 GBM cell line as an unmethylated control; U87, U87 GBM cell line as a methylated control. The representative case (patient 1) is shown. Surg., primary tumors at surgery; Autop., recurrent tumor obtained at autopsy following the treatment with the GSK3β-inhibiting drugs.

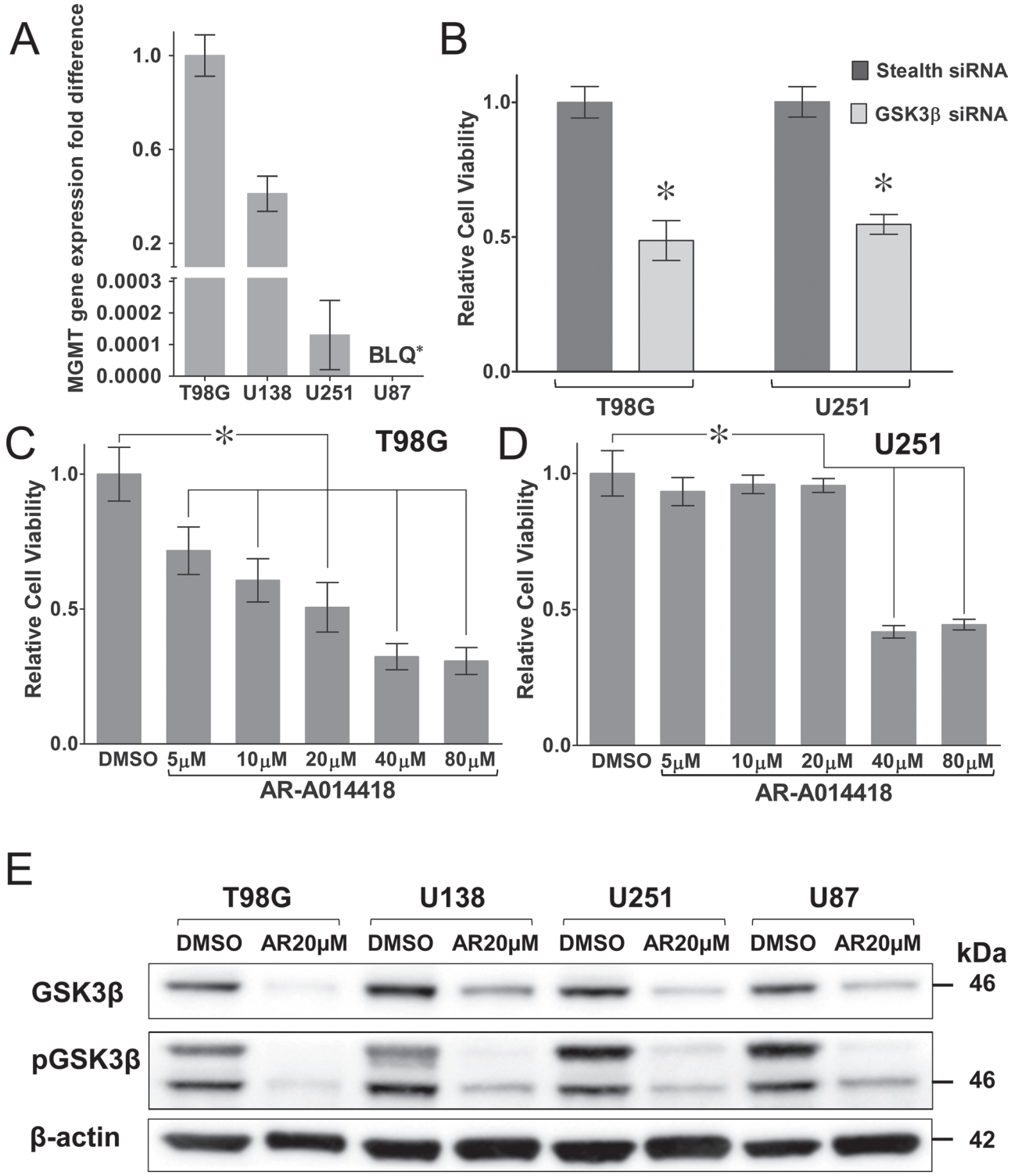

Fig. 2. (**A**) A comparison of the levels of MGMT gene expression in T98G, U138, U251 and U87 GBM cells by QRT–PCR with primers specific to MGMT. The relative value of MGMT messenger RNA expression in T98G was scored as 1.0. *BLQ, below the limit of quantitation; bars show standard deviations in the data. The figure shows the data from three independent experiments. (**B**) The effect of GSK3β–RNA interference on GBM cell survival. Values of relative cell viability were measured by the AlamarBlue assay and compared between T98G and U251 cells transfected with GSK3β-specific and non-specific siRNA (10 nmol/l each), respectively, for 72 h. The relative viability of the cells treated with non-specific siRNA was scored as 1.0. $*P = 0.002$; Mann–Whitney *U*-test, bars show standard deviation. The figure shows the data from experiments carried out in sextuplicates. (**C** and **D**) The relative cell viability of T98G and U251 cells was measured by the AlamarBlue assay and compared between cells treated with DMSO (control) or AR-A014418 (5, 10, 20, 40 or 80 μmol/l) for 144 h. The relative viability of the cells treated with DMSO was scored as 1.0. $*P < 0.05$; Mann–Whitney *U*-test, bars show standard deviation. The figure shows the data from experiments carried out in sextuplicates. (**E**) The effect of GSK3β inhibitor (AR-A014418) on the expression of total and tyrosine 216-phosphorylated GSK3β. Equal amounts of whole-cell lysates from T98G, U138, U251 and U87 cells treated with DMSO or 20 μmol/l AR-A014418, respectively, for 72 h were analyzed by western blot of total and phosphorylated GSK3β proteins, with β-actin used as loading control. AR, AR-A014418. The figure shows the representative data from three independent western blots.

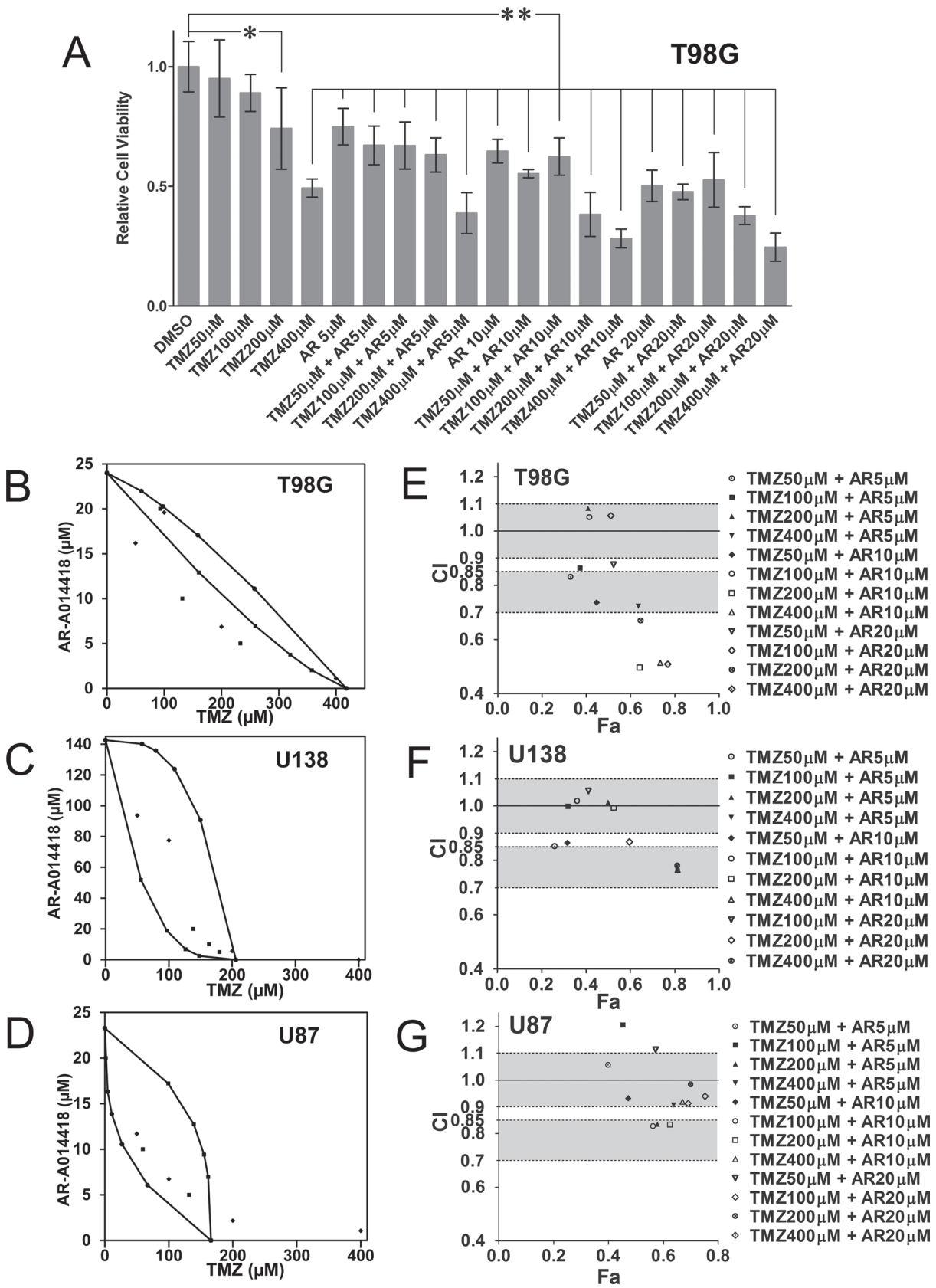

Fig. 3. The combined effect of TMZ and a GSK3β inhibitor (AR-A014418) on GBM cells. (**A**) The relative cell viability of T98G cells after treatment for 144 h with TMZ (50, 100, 200 and 400 μmol/l) or AR-A014418 (5, 10 and 20 μmol/l), alone or in different combinations shown below the panel, measured by the AlamarBlue assay. The relative viability of the cells treated with DMSO alone was scored as 1.0. $*P < 0.05$, $**P < 0.01$, AR, AR-A014418; Mann–Whitney *U*-test, compared with DMSO-treated cells; bars show standard deviation. (**B–G**) A comparison of combined effect of TMZ (50, 100, 200 and 400 μmol/l) and AR-A014418 (5, 10 and 20 μmol/l) on T98G, U138 and U87 cells. (B–D) Classic isobologram method. The IC_{50} values of the combination therapy by TMZ and AR-A014418 determined by the AlamarBlue assay were plotted (TMZ IC_{50}, closed square; AR-A014418 IC_{50}, closed diamond).

Capacity complementary DNA Reverse Transcription Kit (Applied Biosystems). Quantitative reverse transcriptase–polymerase chain reaction (QRT–PCR) was performed using a LightCycler FastStart DNA MasterPlus SYBRGreen kit (Roche Diagnostics GmbH) with the respective sense and antisense primers for MGMT and glyceraldehyde 3-phosphate dehydrogenase (all from Sigma) that span exon–exon junctions preventing amplification of contaminating genomic DNA. QRT–PCR was carried out in a LightCycler 1.5 as described previously (25). QRT–PCR was done with the following set of primers for MGMT (NM_002412.3): forward primer, 5′-CCTGGCTGAATGCCTATTTC-3′ and reverse primer, 5′-TGTCTGGTGAACGACTCTTG-3′ (amplicon size: 100 bp); and for glyceraldehyde 3-phosphate dehydrogenase (NM_002046.3): forward primer, 5′-CTCCTCCTGTTCGACAGTCA-3′ and reverse primer, 5′-CCAATACGACCAAATCCGTTG-3′ (amplicon size: 112 bp). All primers other than the MGMT forward primer (26) were designed with Primer-BLAST software (http://www.ncbi.nlm.nih.gov/tools/primer-blast/). The QRT–PCR reaction protocol consisted of an initial denaturation step at 95°C for 10 min followed by 40 cycles of 95°C for 10 s, 60°C for 10 s and 72°C for 5 s. LightCycler Software 4.1 was used to analyze the QRT–PCR data. Ct was determined and relative messenger RNA expression was calculated using the ΔC_T method described by the manufacturer using glyceraldehyde 3-phosphate dehydrogenase as a calibrator gene.

Chromatin immunoprecipitation assay

To assess c-Myc and DNA (cytosine-5)-methyltransferase 3A (DNMT3A) binding to the MGMT promoter chromatin immunoprecipitation (ChIP) assay was performed utilizing a SimpleChIP Enzymatic Chromatin IP Kit (Cell Signaling Technology) as described previously (27). Briefly, two-step protein and chromatin fixation was performed with N-hydroxysuccinimide ester-ester cross-linking reagent ethylene glycol bis(succinimidylsuccinate) (EGS) (Pierce Biotechnology, Rockford, IL) and formaldehyde (Sigma). EGS stock solution was added to T98G and U138 cells to a final concentration of 2 mM and rapidly mixed. Cells were fixed with EGS for 45 min at room temperature. After EGS fixation, the cells were washed three times with phosphate-buffered saline. Ten milliliters of a freshly prepared 1% (v/v) solution of formaldehyde in phosphate-buffered saline, pH 8.0, were added, and the cells were incubated at room temperature for 15 min and processed according to the SimpleChIP Enzymatic Chromatin IP Kit protocol. We used anti-c-Myc (Cell Signaling Technology), anti-DNMT3A antibodies (Imgenex) and anti-histone H3 (D2B12) XP antibody (Cell Signaling Technology) as a positive control or anti-FLAG M2 antibody (Sigma) as an unrelated antibody as a negative control. Immunoprecipitated DNA was analyzed by qPCR using LightCycler 1.5 with a LightCycler FastStart DNA MasterPlus SYBRGreen kit and the primers for E-box localized in the human MGMT promoter (NT_008818.16 2498978-83). We designed these primers and tested their specificity with Primer-BLAST software. Sequences of the primers used are available on request. The LightCycler Software 4.1 was used to evaluate the qPCR data. Ct were determined and % input values were calculated.

Statistical analyses

Statistical analyses were done using Mann–Whitney *U*-test and Kruskal–Wallis one-way analysis of variance test. $P < 0.05$ was considered significant.

Results

Inhibition of glycogen synthase phosphorylation by GSK3β-inhibiting drugs

To assess the effect of the GSK3β-inhibiting drugs in the patients with recurrent GBM, immunohistochemistry was performed on tumor specimens. The primary tumor and the recurrent tumor tissues in all patients were positive for glycogen synthase (GS) (Supplementary Figure S1, available at *Carcinogenesis* Online). Phosphorylation of GS reflects GSK3β activity since GS is the primary substrate for GSK3β (8). Immunohistochemistry demonstrated that the cytoplasm of tumor cells was strongly positive for p-GS^{S641} in patients 1 and 2 (Figure 1A, a and c). However, staining was weak in the tumors obtained by autopsy (Figure 1A, b and d). In contrast, p-GS^{S641} was preserved in autopsy specimen in patient 3 (Supplementary Figure S2, available at *Carcinogenesis* Online). This result suggests that the GSK3β-inhibiting drugs function in the tumor cells of the patients.

Changes in the expression and promoter methylation of MGMT in the tumors

The level of MGMT expression was compared by immunohistochemistry of the primary tumor and the recurrent tumor tissues from the same patients treated with the GSK3β-inhibiting drugs (Figure 1B and C). Tumor cells were strongly positive for MGMT in primary tumors (Figure 1B, a and c), whereas weak expression was observed in the tumors obtained at autopsy in patients 1 and 2, respectively (Figure 1B, b and d). In contrast, MGMT was detected both in primary tumor and autopsy specimen in patient 3 (Supplementary Figure S3, available at *Carcinogenesis* Online). This suggests that MGMT was downregulated in response to the inhibition of GSK3β in the tumor tissues.

With the findings shown above, we hypothesized that treatment with the GSK3β-inhibiting drugs decreased MGMT expression in the tumors by epigenetic silencing of its gene. To address this, a MSP assay was performed to examine the methylation status of the MGMT promoter in the tumor tissues. Although the MGMT promoter was unmethylated in the primary tumors at surgery, it became methylated in the tumors obtained at autopsy in patient 1 (Figure 1D).

MGMT gene expression in glioma cells

We investigated the mechanism of MGMT silencing by GSK3β inhibition. Initially, we screened for the glioma cell lines T98G, U138, U251 and U87. Basal MGMT gene expression was determined by QRT–PCR. T98G, U138 and U251 cell lines expressed the MGMT gene transcripts, whereas U87 showed no detectable MGMT gene expression (Figure 2A).

GSK3β inhibition and glioma cell viability

To determine the function of GSK3β in the glioma cell lines, we used siRNA to specifically knockdown endogenous GSK3β. The specific reduction of GSK3β by siRNA was determined in our previous study (10). Depletion of GSK3β, confirmed by western blot analysis (Supplementary Figure S4, available at *Carcinogenesis* Online), significantly decreased cell viability in T98G and U251 cells (Figure 2B). To further assess the effect of inhibition of GSK3β activity, we treated the cells with dose-escalating AR-A014418. Cell viability was decreased by AR-A014418 treatment in a dose-dependent manner in T98G cells (Figure 2C). IC_{50} was ~20 μmol/l. Decreased viability by AR-014418 was also observed in U251 cells (Figure 2D). Consistently with previous study showing depletion of GSK3β by AR-A014418 treatment (28), depletion of total and tyrosine 216-phosphorylated GSK3β by AR-A014418 was observed in glioma cells by western blot analysis (Figure 2E). These data showed that GSK3β inhibition attenuates viability in T98G and U251 cells. According to the range of linear dose-dependent response in T98G cells, a 5–20 μmol/l dose range of AR-A014418 was used to assess combination treatment with TMZ.

Combined effect of GSK3β inhibitor and TMZ in GBM cells

To investigate whether GSK3β inhibition enhances TMZ effect, T98G, U138 and U87 cells were treated with different doses of TMZ or AR-A014418, alone or in combination. Compared with U138, U87 (Supplementary Figure S5, available at *Carcinogenesis* Online) and U251 as shown previously (10), T98G cells were much

←

A 5 and 10 μmol/l of AR-A014418 and 50 and 200 μmol/l of TMZ appeared to be under the *envelope of additivity* (continuous line with closed square and continuous line with closed circle, respectively), showing synergistic action against T98G cells. IC_{50} values for combination treatment, which are inside the envelope of additivity, reveal the additive action of TMZ and AR-A014418 treatment against GBM cells. (E–G) Median dose-effect analysis. Dose-normalized combination indices (CI) of the combination therapy by TMZ and AR-A014418 were plotted. CI values for combination treatment within intervals 0.3–0.7, 0.7–0.85, 0.85–0.90 and 0.90–1.10 reveal synergism, moderate synergism, slight synergism and nearly additive action, respectively, of TMZ and AR-A014418 treatment against GBM cells. Fa, affected cell fraction. The figure shows the data from experiments carried out in sextuplicates.

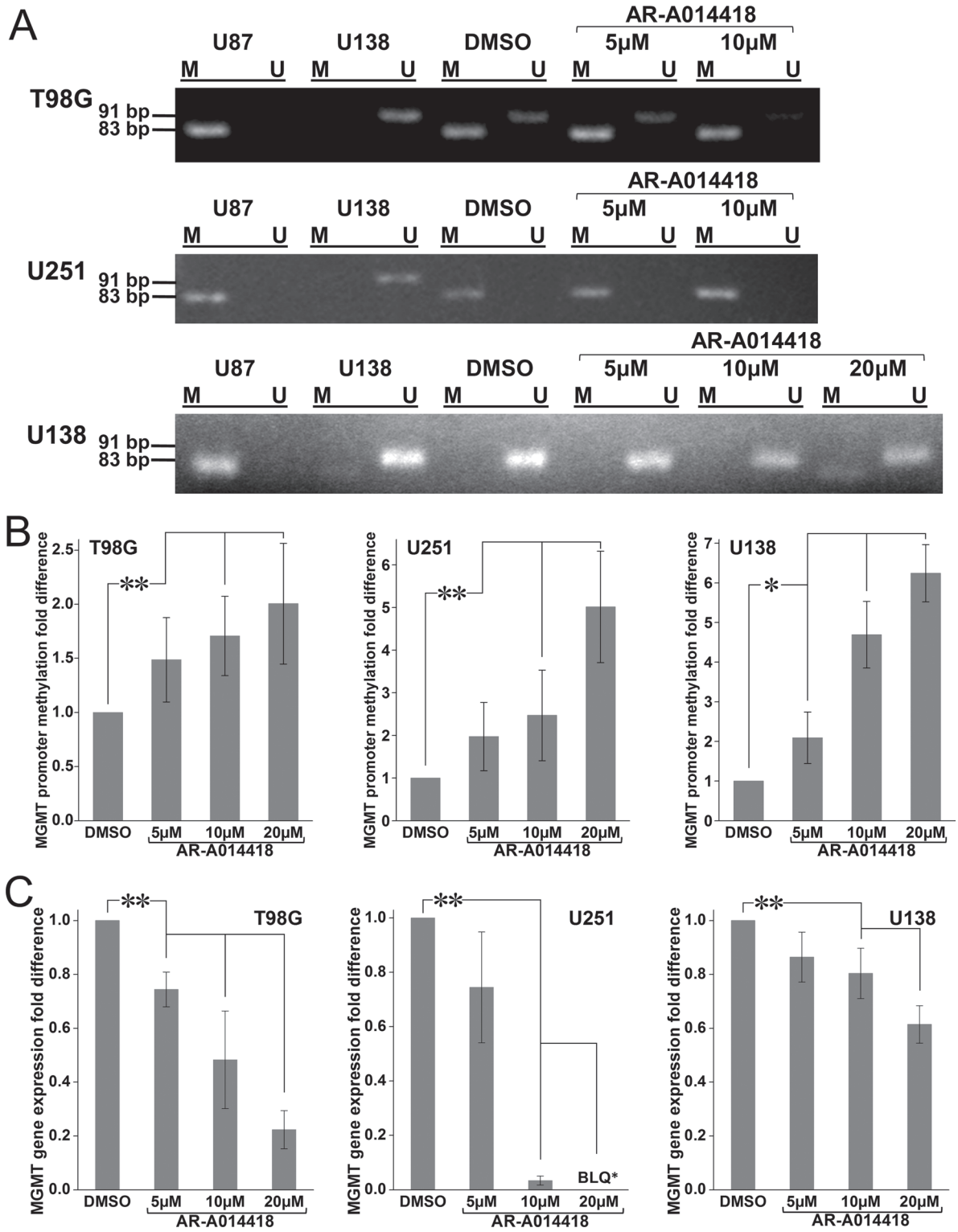

Fig. 4. (**A**) Changes in MGMT gene methylation status in GBM cells by GSK3β inhibition. The effect of GSK3β inhibition with 5, 10 or 20 μmol/l of AR-A014418 for 72 h on the methylation status of the MGMT promoter in T98G, U251 and 138 cells was observed by MSP assay. PCR products in the M lanes and U lanes indicate methylated and unmethylated status of the MGMT promoter, respectively. U87, U87 GBM cell line as a methylated control; U138, U138 GBM cell line as an unmethylated control; AR, AR-A014418. (**B**) The effect of GSK3β inhibition on methylation status of the MGMT promoter examined with MethyLight assay in T98G, U251 and U138 cells treated for 72 h with DMSO or AR-A014418 (5, 10 or 20 μmol/l). qPCR of bisulfite-converted DNA with the primers and probes specific to the methylated fraction of the MGMT promoter. The level of MGMT promoter methylation in the cells treated with DMSO was scored as 1.0. $^{*}P < 0.05$, $^{**}P < 0.01$, AR, AR-A014418; Mann–Whitney *U*-test, bars show standard deviation. The figure shows the data from three independent experiments. (**C**) QRT–PCR analysis of the effect of GSK3β inhibition on MGMT gene expression in T98G, U251 and U138 cells treated with DMSO or AR-A014418 (5, 10 or 20 μmol/l), respectively, for 72 h. The level of MGMT messenger RNA expression in the cells treated with DMSO was scored as 1.0. *BLQ, below the limit of quantitation. $^{**}P < 0.01$; Mann–Whitney *U*-test, bars show standard deviation. The figure shows the data from three independent experiments.

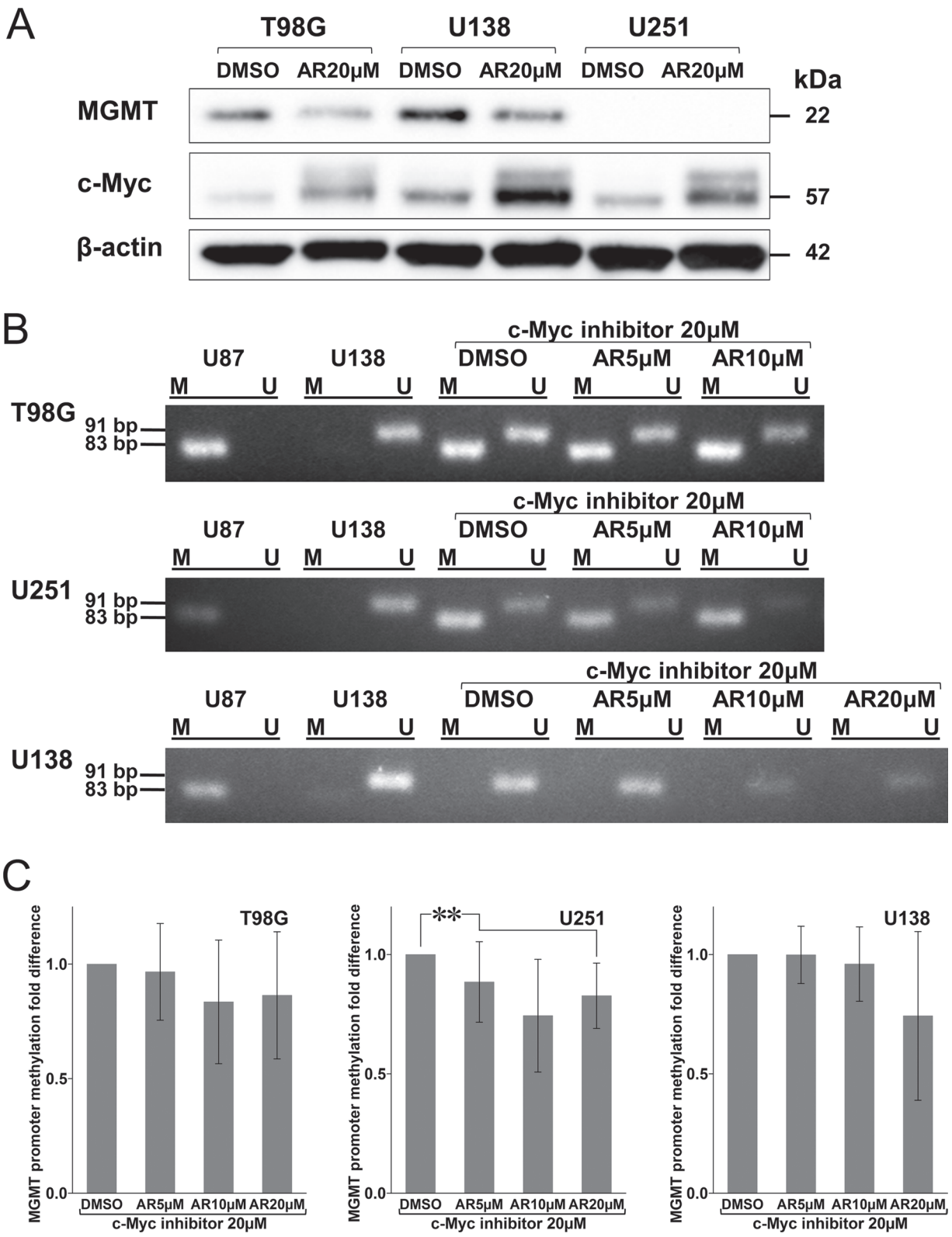

Fig. 5. (**A**) The effect of GSK3β inhibitor (AR-A014418) on the expression of MGMT and c-Myc. Equal amounts of whole-cell lysates from T98G, U138 and U251 cells treated with DMSO or 20 μmol/l AR-A014418, respectively, for 72 h were analyzed by western blot of c-Myc and MGMT proteins, with β-actin used as loading control, AR, AR-A014418. The figure shows the representative data from three independent western blots. (**B**) Changes in MGMT gene methylation status in GBM cells by GSK3β and c-Myc inhibition. The effect of combination of DMSO–AR-A014418 (5, 10 or 20 μmol/l) and c-Myc inhibitor 20 μmol/l for 72 h on the methylation status of the MGMT promoter in T98G, U251 and U138 cells was observed by MSP assay. PCR products in the M lanes and U lanes indicate methylated and unmethylated status of the MGMT promoter, respectively. U87, U87 GBM cell line as a methylated control; U138, U138 GBM cell line as an unmethylated control; AR, AR-A014418. (**C**) The effect of GSK3β and c-Myc inhibition on methylation status of the MGMT promoter examined with MethyLight assay in T98G, U251 and U138 cells treated for 72 h with combination of DMSO–AR-A014418 (5, 10 or 20 μmol/l) and c-Myc inhibitor 20 μmol/l. qPCR of bisulfite-converted DNA with the primers and probes specific to the methylated fraction of the MGMT promoter. The level of MGMT promoter methylation in the cells treated with DMSO was scored as 1.0. $^{**}P < 0.01$, AR, AR-A014418; Mann–Whitney *U*-test, bars show standard deviation. The figure shows the data from three independent experiments.

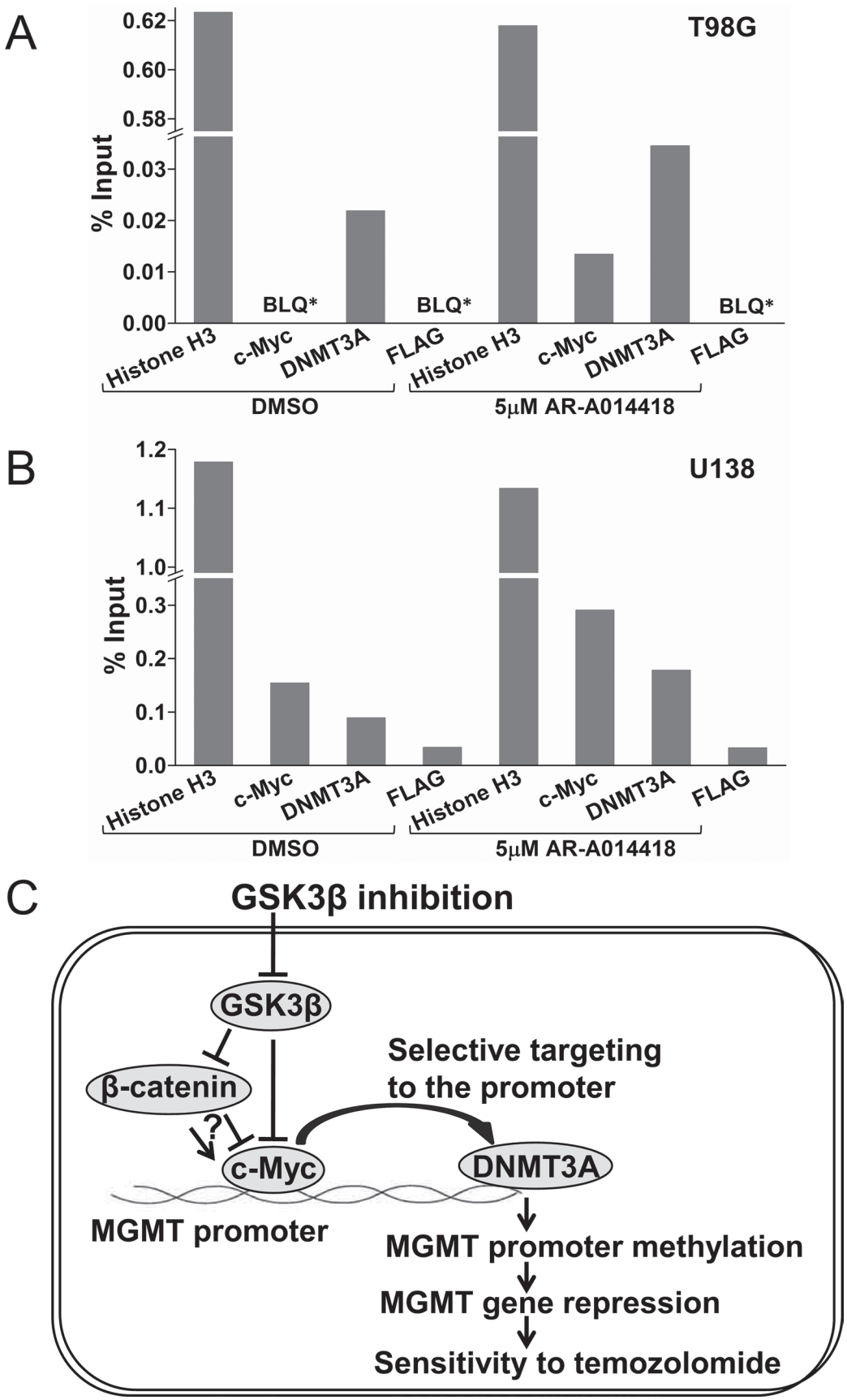

Fig. 6. Epigenetic silencing of MGMT expression by GSK3β inhibition. (**A** and **B**) Comparison by ChIP assay of the binding of histone H3, c-Myc, DNMT3A and FLAG to the E-box site in the MGMT promoter between the GBM cells treated with DMSO or with a GSK3β inhibitor (AR-A014418). T98G and U138 cells were treated for 72 h with DMSO or 5 μmol/l of AR-A014418. The amount of DNA coprecipitated with the antibody to each molecule was measured by

more chemoresistant to TMZ (Figure 3A), which is consistent with a higher basal level of MGMT expression (Figure 2A). The combination of low-dose AR-A014418 and TMZ significantly reduced cell viability compared with the treatment with TMZ or low-dose AR-A014418 alone (Figure 3A). Classic isobologram analysis and median dose-effect analysis were performed to evaluate whether low-dose AR-A014418 potentiates TMZ effect against GBM cells. The data obtained showed mainly synergistic antitumor effect of low-dose AR-A014418 (5, 10 and 20 μmol/l) in combination with TMZ in T98G cells (Figure 3B and E), whereas U138 demonstrating lower basal MGMT expression (Figure 2A) showed additive and moderate synergistic effect (Figure 3C and F), while mainly additive effect was noted in U87 (Figure 3D and G) and in U251 in our previous report (10) with undetectable and low MGMT expression, respectively (Figure 2A).

Effect of GSK3β inhibition on MGMT promoter methylation status and gene expression

To investigate the influence of GSK3β inhibition on MGMT promoter methylation, a MSP assay was performed in T98G, U251 and U138 cells expressing MGMT (Figure 2A). AR-A014418 treatment decreased or ablated unmethylated MGMT promoter in T98G, increased methylated MGMT promoter in U251 and decreased unmethylated MGMT promoter in U138 cells revealing methylated MGMT promoter at 20 μmol/l (Figure 4A). MSP assay data were confirmed by the MethyLight assay showing that GSK3β inhibition increased methylation of CpG islands in the MGMT promoter in T98G, U251 and U138 cells after treatment with AR-A014418 (Figure 4B). Consistent with the changes in methylation levels, GSK3β inhibition by AR-A014418 decreased the levels of MGMT gene expression in T98G, U138 and U251 cells as measured by QRT–PCR (Figure 4C). Consistently, MGMT protein expression was decreased by AR-A014418 treatment in T98G and U138, whereas MGMT was undetectable in U251 cells with low MGMT expression (Figures 2A and 5A).

Effect of GSK3β inhibition on c-Myc and DNMT3A binding to the MGMT promoter

To investigate the molecules that are responsible for the changes in MGMT promoter methylation status, we focused on c-Myc signaling. c-Myc is a good candidate since GSK3β inhibition increases c-Myc expression in U251 (12), T98G, U138 (Figure 5A and Supplementary Figure S6, available at *Carcinogenesis* Online) and U87 cells (I.V.Pyko, unpublished results), as shown by western blot analysis and QRT–PCR (I.V.Pyko, unpublished results).

To determine if the effect of GSK3β inhibition on MGMT promoter methylation is mediated by c-Myc signaling, we performed MSP assay and MethyLight assay in T98G, U251 and U138 cell lines treated with combination of DMSO–AR-A014418 and c-Myc inhibitor. As shown in Figure 5B, the c-Myc inhibitor caused increase/appearance of unmethylated MGMT promoter in T98G and U251 cells and ablated AR-A014418-induced MGMT promoter methylation (Figure 4A) in U138 cells in MSP assay, suggesting that c-Myc plays a role in MGMT promoter methylation in the GBM cells. Comparing with the data shown in Figure 4A, concomitant treatment with the c-Myc inhibitor and AR-A014418 maintained the fraction of unmethylated MGMT promoter in these cells. MethyLight assay demonstrated that c-Myc inhibitor abrogated the AR-A014418-induced increase of MGMT promoter methylation in all cells (Figure 5C). The results of MSP and MethyLight assays collectively suggest that c-Myc-mediated signaling is responsible for MGMT promoter methylation induced by the GSK3β inhibitor in the GBM cells.

c-Myc is a target for β-catenin-mediated gene transcription by T-cell factor/lymphoid-enhancer factor (29). We have shown previously that GSK3β inhibition increases β-catenin expression in T98G and U251 cells (10). To determine if c-Myc expression is increased via β-catenin signaling in the glioma cell lines, we used siRNA to specifically knockdown endogenous β-catenin. Depletion of β-catenin, confirmed by western blot analysis (Supplementary Figure S7, available at *Carcinogenesis* Online), resulted in decreased c-Myc expression in U138; however, in T98G and U251, β-catenin depletion increased c-Myc expression and produced no significant changes in U87 cells (Supplementary Figure S7, available at *Carcinogenesis* Online). It suggests that the regulation of c-Myc by β-catenin under GSK3β inhibition is cell dependent.

c-Myc is known to selectively target DNMT3A to the promoter of the gene, resulting in DNA methylation *de novo* and silencing of the targeted promoter (30). DNMT3A protein expression was not changed by GSK3β siRNA (Supplementary Figure S8, available at *Carcinogenesis* Online), suggesting that changes in DNMT3A expression are not involved in regulation of MGMT promoter methylation via DNMT3A in GBM cells.

We examined possible interaction between c-Myc and DNMT3A by the ChIP assay. We chose T98G and U138 cells since T98G is highly resistant to TMZ due to the high basal level of MGMT gene expression (Figure 2A), and the observed synergistic effect of combined treatment with AR-A014418 and TMZ against T98G and U138 cells (Figure 3B, C, E and F) was accompanied by a decrease in unmethylated MGMT promoter after AR-A014418 treatment (Figure 4A). In ChIP assay, c-Myc binding to the E-box transcription factor-binding site in the MGMT promoter was on detectable level in U138 and below the limit of quantitation in T98G in DMSO-treated control, whereas AR-A014418 treatment increased c-Myc binding to the same site in the MGMT promoter in both cell lines. This finding was accompanied by increased DNMT3A binding to the same region in the MGMT promoter in T98G and U138 cells (Figure 6A and B). These data suggest that, in response to GSK3β inhibition, c-Myc recruits DNMT3A to the MGMT promoter, which increases its methylation level in T98G and U138 cells.

Discussion

In our clinical research, the GSK3β-inhibiting drugs inhibited GS phosphorylation and decreased MGMT expression, a predictor for resistance to TMZ, in tumor cells in patients with recurrent GBM. Consistent with these findings, the status of the MGMT promoter changed from unmethylated to methylated after treatment with GSK3β-inhibiting drugs. These data suggest that GSK3β inhibition decreases MGMT production in GBM affecting the methylation status of the MGMT promoter. This observation in patient tumors was extrapolated by novel findings in this study, demonstrating that GSK3β inhibition in GBM cells induced c-Myc-dependent recruitment of DNMT3A, leading to MGMT promoter methylation and consequent silencing of MGMT expression (Figure 6A and B).

In our study, T98G and U138 cells appeared to be highly resistant to TMZ treatment, and this can be attributed to high MGMT gene expression level in these cell lines. It is consistent with previous reports asserting that T98G has the highest MGMT expression level among 10 GBM cell lines (7) and is extremely resistant to TMZ (31,32). Here, we showed that GSK3β inhibition enhanced TMZ effect in T98G cells to sensitivity levels seen in TMZ-sensitive cell lines (10). The synergistic effect observed for the combination treatment of GSK3β inhibitor with low-dose TMZ (50 μmol/l) may be considered in future clinical applications as it is within the TMZ therapeutic window for systemic administration (33,34).

←
qPCR with a set of primers specific to the E-box transcription factor-binding site in the MGMT promoter. *BLQ, below the limit of quantitation. The figure shows the representative data from two independent immunoprecipitations. (**C**) Regulation of MGMT expression by GSK3β signaling. GSK3β inhibition results in c-Myc activation directly and via activation of β-catenin-mediated signaling, which consequently increases recruitment of DNMT3A by c-Myc to the MGMT promoter, thus increasing *de novo* DNA methylation in the MGMT promoter. The methylated status of the MGMT promoter increases the sensitivity of GBM to TMZ.

c-Myc is an important factor in cell proliferation that enables G_1/S cell cycle progression (35). Despite its role in cell proliferation, several studies show an essential role for c-Myc in apoptosis (36,37). A previous report demonstrated that c-Myc has a suppressive effect in human GBM cells, as c-Myc upregulation is associated with increased apoptosis (12). GSK3β has also been reported to phosphorylate (38) and destabilize c-Myc (11) and GSK3β inhibition in glioma cells along with the upregulation of Ser^{62} phosphorylation and downregulation of Thr^{58} phosphorylation of c-Myc, results in increased c-Myc expression (12). Taken together, c-Myc expression is increased in GBM cells by GSK3β inhibition via its effects on c-Myc phosphorylation and in some cell lines its effect on β-catenin mediated gene transcription.

Considering the role of c-Myc in apoptosis (12), additive effect of GSK3β inhibition and TMZ in U87 showing undetectable MGMT expression (Figure 3D and G) can be explained by c-Myc upregulation (I.V.Pyko, unpublished results). Moreover, TMZ induces G_2/M arrest decreasing its effect (39) by retention of proliferative capacity in U87 cells (40). Accordingly, our laboratory previously have shown cyclin D1 upregulation in U87 by GSK3β inhibition (10), suggesting that GSK3β inhibition can enhance TMZ effect in U87 cells reducing TMZ-induced G_2/M arrest.

It is known that c-Myc can silence gene expression by active recruitment of corepressor proteins and that it can target DNMT3A selectively to the promoter of the gene (30). However, there are no studies showing binding of c-Myc to the MGMT promoter (41), despite the presence of an E-box transcription factor-binding site in the MGMT promoter. In this study, we hypothesized that a high expression level of c-Myc in GBM cells induced by GSK3β inhibition induces c-Myc binding to the E-box, resulting in transcriptional repression via recruitment of DNMT3A.

Our ChIP assay demonstrated for the first time that c-Myc binds to the MGMT promoter in intact cells and that c-Myc and DNMT3A binding to the MGMT promoter increases after AR-A014418 treatment. The mediation of c-Myc for recruitment of DNMT3A to the MGMT promoter was confirmed by comparison of data from the conventional ChIP assay, which includes a one-step protein and chromatin fixation with formaldehyde (I.V.Pyko, unpublished results) and data from the ChIP assay with a two-step protein and chromatin fixation shown in this study. Conventional ChIP assay, which effectively detects direct protein–DNA binding, did not reveal detectable DNMT3A binding to the MGMT promoter. In contrast, ChIP assay with a two-step protein and chromatin fixation provides effective detection of both direct protein–DNA binding and indirect protein–protein–DNA binding (27). Consequently, our ChIP assay with a two-step protein and chromatin fixation showed detectable DNMT3A binding to the MGMT promoter with an increased binding level in GBM cells treated with AR-A014418. This was consistent with an increase in c-Myc binding after AR-A014418 treatment, suggesting recruitment of DNMT3A by c-Myc to the MGMT promoter (Figure 6A and B).

Based on our data, we speculate that GSK3β inhibition eliminates the suppressive effect of GSK3β on c-Myc expression by the effects on c-Myc phosphorylation, which subsequently increases recruitment of DNMT3A by c-Myc to the MGMT promoter in GBM cells. The interaction between c-Myc and DNMT3A would then activate DNA methyltransferase, which increases local *de novo* DNA methylation in the CpG islands of the MGMT promoter. MGMT promoter methylation silences MGMT gene expression, and this finally sensitizes GBM cells to TMZ (Figure 6C). The provided data will facilitate the development of an optimal combination of GSK3β inhibitor and alkylating agents for their use in the treatment of patients with GBM. Further *in vivo* research is needed to optimize combination regimens of TMZ and GSK3β inhibitor for the treatment of refractory GBM.

Supplementary material

Supplementary Figures S1–S8 can be found at http://carcin.oxfordjournals.org/

Funding

Grant-in-Aid for Scientific Research from the Japan Society for the Promotion of Science (C-23592117 to M.N.); Foundation for Promotion of Cancer Research to M.N.; Kobayashi Foundation for Cancer Research to M.N.

Conflict of Interest Statement: None declared.

References

1. DeAngelis,L.M. (2001) Brain tumors. *N. Engl. J. Med.*, **344**, 114–123.
2. Lefranc,F. *et al.* (2005) Possible future issues in the treatment of glioblastomas: special emphasis on cell migration and the resistance of migrating glioblastoma cells to apoptosis. *J. Clin. Oncol.*, **23**, 2411–2422.
3. Stewart,L.A. (2002) Chemotherapy in adult high-grade glioma: a systematic review and meta-analysis of individual patient data from 12 randomised trials. *Lancet*, **359**, 1011–1018.
4. Miyashita,K. *et al.* (2009) An emerging strategy for cancer treatment targeting aberrant glycogen synthase kinase 3 beta. *Anticancer. Agents Med. Chem.*, **9**, 1114–1122.
5. Nakada,M. *et al.* (2011) The pivotal role of GSK3β in glioma biology. In Garami,M. (ed.) *Molecular Targets of CNS Tumors*. InTech, Croatia, pp. 567–590.
6. Hegi,M.E. *et al.* (2005) MGMT gene silencing and benefit from temozolomide in glioblastoma. *N. Engl. J. Med.*, **352**, 997–1003.
7. Costello,J.F. *et al.* (1994) Graded methylation in the promoter and body of the O^6-methylguanine DNA methyltransferase (MGMT) gene correlates with MGMT expression in human glioma cells. *J. Biol. Chem.*, **269**, 17228–17237.
8. Jope,R.S. *et al.* (2004) The glamour and gloom of glycogen synthase kinase-3. *Trends Biochem. Sci.*, **29**, 95–102.
9. Bhat,R. *et al.* (2003) Structural insights and biological effects of glycogen synthase kinase 3-specific inhibitor AR-A014418. *J. Biol. Chem.*, **278**, 45937–45945.
10. Miyashita,K. *et al.* (2009) Potential therapeutic effect of glycogen synthase kinase 3 beta inhibition against human glioblastoma. *Clin. Cancer Res.*, **15**, 887–897.
11. Gregory,M.A. *et al.* (2003) Phosphorylation by glycogen synthase kinase-3 controls c-myc proteolysis and subnuclear localization. *J. Biol. Chem.*, **278**, 51606–51612.
12. Kotliarova,S. *et al.* (2008) Glycogen synthase kinase-3 inhibition induces glioma cell death through c-MYC, nuclear factor-kappaB, and glucose regulation. *Cancer Res.*, **68**, 6643–6651.
13. Louis,D.N. *et al.* (2007) The 2007 WHO classification of tumours of the central nervous system. *Acta Neuropathol.*, **114**, 97–109.
14. Yoshida,Y. *et al.* (2010) Sphingosine-1-phosphate receptor type 1 regulates glioma cell proliferation and correlates with patient survival. *Int. J. Cancer*, **126**, 2341–2352.
15. Wauthoz,N. *et al.* (2010) *In vivo* assessment of temozolomide local delivery for lung cancer inhalation therapy. *Eur. J. Pharm. Sci.*, **39**, 402–411.
16. Nakada,M. *et al.* (2005) EphB2/R-Ras signaling regulates glioma cell adhesion, growth, and invasion. *Am. J. Pathol.*, **167**, 565–576.
17. Breinholt,V. *et al.* (1998) Detection of weak estrogenic flavonoids using a recombinant yeast strain and a modified MCF7 cell proliferation assay. *Chem. Res. Toxicol.*, **11**, 622–629.
18. Steel,G.G. *et al.* (1979) Exploitable mechanisms in combined radiotherapy-chemotherapy: the concept of additivity. *Int. J. Radiat. Oncol. Biol. Phys.*, **5**, 85–91.
19. Chou,T.C. *et al.* (1984) Quantitative analysis of dose-effect relationships: the combined effects of multiple drugs or enzyme inhibitors. *Adv. Enzyme Regul.*, **22**, 27–55.
20. Chou,T.C. (2006) Theoretical basis, experimental design, and computerized simulation of synergism and antagonism in drug combination studies. *Pharmacol. Rev.*, **58**, 621–681.
21. Palmisano,W.A. *et al.* (2000) Predicting lung cancer by detecting aberrant promoter methylation in sputum. *Cancer Res.*, **60**, 5954–5958.
22. Suzuki,T. *et al.* (2011) The correlation between promoter methylation status and the expression level of O6-methylguanine-DNA methyltransferase in recurrent glioma. *Jpn. J. Clin. Oncol.*, **41**, 190–196.
23. Eads,C.A. *et al.* (2001) Epigenetic patterns in the progression of esophageal adenocarcinoma. *Cancer Res.*, **61**, 3410–3418.
24. Weisenberger,D.J. *et al.* (2005) Analysis of repetitive element DNA methylation by MethyLight. *Nucleic Acids Res.*, **33**, 6823–6836.
25. Mariani,L. *et al.* (2001) Identification and validation of P311 as a glioblastoma invasion gene using laser capture microdissection. *Cancer Res.*, **61**, 4190–4196.

26. Rolhion,C. *et al.* (1999) O(6)-methylguanine-DNA methyltransferase gene (MGMT) expression in human glioblastomas in relation to patient characteristics and p53 accumulation. *Int. J. Cancer*, **84**, 416–420.
27. Nowak,D.E. *et al.* (2005) Two-step cross-linking method for identification of NF-kappaB gene network by chromatin immunoprecipitation. *Biotechniques*, **39**, 715–725.
28. Bilim,V. *et al.* (2009) Glycogen synthase kinase-3: a new therapeutic target in renal cell carcinoma. *Br. J. Cancer*, **101**, 2005–2014.
29. Baek,S.H. *et al.* (2003) Regulated subset of G1 growth-control genes in response to derepression by the Wnt pathway. *Proc. Natl Acad. Sci. USA*, **100**, 3245–3250.
30. Brenner,C. *et al.* (2005) Myc represses transcription through recruitment of DNA methyltransferase corepressor. *EMBO J.*, **24**, 336–346.
31. Kanzawa,T. *et al.* (2003) Inhibition of DNA repair for sensitizing resistant glioma cells to temozolomide. *J. Neurosurg.*, **99**, 1047–1052.
32. Torres,S. *et al.* (2011) A combined preclinical therapy of cannabinoids and temozolomide against glioma. *Mol. Cancer Ther.*, **10**, 90–103.
33. Ostermann,S. *et al.* (2004) Plasma and cerebrospinal fluid population pharmacokinetics of temozolomide in malignant glioma patients. *Clin. Cancer Res.*, **10**, 3728–3736.
34. Plummer,E.R. *et al.* (2005) Temozolomide pharmacodynamics in patients with metastatic melanoma: DNA damage and activity of repair enzymes O6-alkylguanine alkyltransferase and poly(ADP-ribose) polymerase-1. *Clin. Cancer Res.*, **11**, 3402–3409.
35. Steiner,P. *et al.* (1995) Identification of a Myc-dependent step during the formation of active G1 cyclin-cdk complexes. *EMBO J.*, **14**, 4814–4826.
36. Packham,G. *et al.* (1995) c-Myc and apoptosis. *Biochim. Biophys. Acta*, **1242**, 11–28.
37. Askew,D.S. *et al.* (1991) Constitutive c-myc expression in an IL-3-dependent myeloid cell line suppresses cell cycle arrest and accelerates apoptosis. *Oncogene*, **6**, 1915–1922.
38. Pulverer,B.J. *et al.* (1994) Site-specific modulation of c-Myc cotransformation by residues phosphorylated *in vivo*. *Oncogene*, **9**, 59–70.
39. Hirose,Y. *et al.* (2001) Abrogation of the Chk1-mediated G(2) checkpoint pathway potentiates temozolomide-induced toxicity in a p53-independent manner in human glioblastoma cells. *Cancer Res.*, **61**, 5843–5849.
40. Hirose,Y. *et al.* (2001) p53 effects both the duration of G2/M arrest and the fate of temozolomide-treated human glioblastoma cells. *Cancer Res.*, **61**, 1957–1963.
41. Zeller,K.I. *et al.* (2003) An integrated database of genes responsive to the Myc oncogenic transcription factor: identification of direct genomic targets. *Genome Biol.*, **4**, R69.

Received December 10, 2012; revised April 29, 2013; accepted May 23, 2013